HOMOTOPY PERTURBATION METHOD ANALYSIS TO MHD FLOW OF A RADIATIVE NANOFLUID WITH VISCOUS DISSIPATION AND OHMIC HEATING OVER A STRETCHING POROUS PLATE

by

Hitesh KUMAR *

Department of Information Technology, Ibri College of Technology, Ibri, Oman

Original scientific paper
https://doi.org/10.2298/TSCI150731209K

An analytical study is performed to explore the flow and heat transfer characteristics of nanofluid (Al_2O_3-water and TiO_3-water) over a linearly stretching porous sheet in the presence of radiation, ohmic heating, and viscous dissipation. Homotopy perturbed method is used and complete solution is presented, the results for the nanofluids velocity and temperature are obtained. The effects of various thermophysical parameters on the boundary-layer flow characteristics are displayed graphically and discussed quantitatively. The effect of viscous dissipation on the thermal boundary-layer is seen to be reverse after a fixed distance from the wall, which is very strange in nature and is the result of a reverse flow. The finding of this paper is unique and may be useful for future research on nanofluid.

Key words: *MHD, homotopy perturbation method, nanofluid, viscous dissipation, radiation, ohmic heating, stretching sheet*

Introduction

The MHD boundary-layer flow of an electrically conducting viscous incompressible fluid with a convective surface boundary condition is frequently encountered in many industrial and technological applications such as extrusion of plastics in the manufacture of rayon and nylon, the cooling of reactors, purification of crude oil, textile industry, polymer technology, metallurgy, geothermal engineering, liquid metals and plasma flows, boundary-layer control in aerodynamics, and crystal growth, *etc*.

Nanofluid is inticipeted to describe a fluid in which nanometer-sized particles are suspended in conventional heat transfer base fluids to improve their thermal physical properties. Nanoparticles are made from various materials, such as metals (Cu, Ag, Au, Al, Fe), oxide ceramics (Al_2O_3, CuO, TiO_2), nitride ceramics (AlN, SiN), carbide ceramics (SiC, TiC), semiconductors, carbon nanotubes, and composite materials such as alloyed nanoparticles or nanoparticle core-polymer shell composites. It is well known that, conventional heat transfer fluids, such as oil, water, and ethylene glycol in general, have poor heat transfer properties compared to those of most solids. Nanofluids have enhanced thermophysical properties such as thermal conductivity. Thermal diffusivity, viscosity, and convective heat transfer coefficients compared with those of base fluids like oil or water. Owing to their enhanced properties, nanofluids can be used in a plethora of technical and biomedical applications such as nanofluid coolant: electronics cooling, vehicle cooling, transformer cooling, computers cooling, and electronic devices cooling. Medical applications: magnetic drug targeting, cancer therapy, and safer surgery by

* Author's e-mail: hiteshrsharma@gmail.com

cooling. Process industries, materials, and chemicals: detergency, food and drink, oil and gas, paper and printing and textiles.

Common heat transport fluids such as water, ethylene glycol, end engine oil have limited heat transfer capabilities due to their low heat transfer properties. In contrast, metals have thermal conductivities up to three times higher than these fluids, so it is natural that it would be desired to combine the two substances to produce a heat transfer medium that behaves like a fluid, but has the thermal conductivity of a metal. A mixture of nanosize particle suspended in a base fluid is named nanofluid [1]. The broad ranges of current and future applications involving nanofluids have been given by Wong and Leone [2]. Many researchers [3-9] have studied and reported results on convective heat transfer in nanofluids considering various flow conditions in different geometries. A comprehensive study of convective transport in nanofluids was made by Buongiorno [10]. Kuznetsov and Nield [11] presented a similarity solution of natural convective boundary-layer flow of a nanofluid past a vertical plate. Abu-Nada and Oztop [12] investigated numerically the effect of a Cu-water nanofluid on natural convection heat transfer in an inclined cavity. They used the inclination angle as a control parameter for flow and heat transfer in the cavity.

In addition to magnetic field, one has to consider the effect of viscous dissipation on the boundary-layer flow since this has a direct influence on the heat transfer rate. Gebhart [13] was first to study the problem by taking into account the viscous dissipation and also defined the non-dimensional dissipation parameter. Pantokratoras [14] studied the effect of viscous dissipation in natural convection along a heated vertical plate. Makinde [15] studied the effect of viscous dissipation on boundary-layer flow over a moving flat plate for two types of water-based Newtonian nanofluids containing metallic or non-metallic nanoparticles such as Cu and TiO_2. They observed that the viscous dissipation effect reduces the wall heat transfer rate and enhances the wall mass transfer rate.

The main motive of this paper to present an analytical solution by homotopy perturbation method (HPM), for a problem of nanofluid flows and heat transfer characteristics, over a linearly stretching porous sheet in the presence of radiation, ohmic heating, and viscous dissipation.

Formulation and solution of problem

Consider a 2-D forced convection boundary-layer flow of an incompressible viscous nanofluid over a stretching porous sheet, fig. 1. The fluid flow is in the influence of viscous dissipation, radiation, ohmic heating and a uniform transverse magnetic field of strength, B_0, (applied parallel to the y-axis). It is assumed that the induced magnetic field and the external electric field are negligible, the base fluid and the nanoparticles are in thermal equilibrium and no slip occurs between them. The flow is considered to be in x-direction which is chosen along the sheet and the y-axis normal to it. The sheet issues from a thin slit at the origin, it is assumed that the speed of a point on the plate is proportional its distance from the slit. Since the length of the sheet is supposed to be large hence fluid-flow extends to infinity, therefore, all physical variables are independent of x and hence functions of y only. The general equations governing the nanofluid flow are:

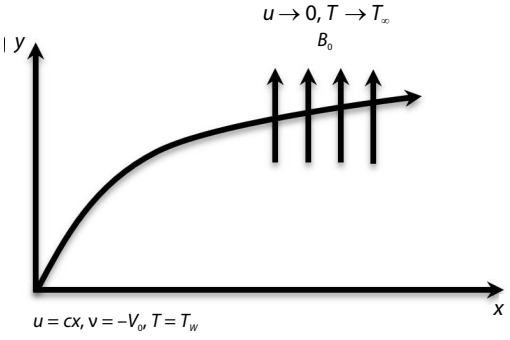

Figure 1. Physical model and co-ordinate system

$$\frac{\partial u}{\partial x}+\frac{\partial v}{\partial y}=0 \tag{1}$$

$$u\frac{\partial u}{\partial x}+v\frac{\partial u}{\partial y}=\frac{1}{\rho_{\mathrm{nf}}}\left(\mu_{\mathrm{nf}}\frac{\partial^2 u}{\partial y^2}-\frac{\mu_{\mathrm{nf}}}{K}u-\sigma B_0^2 u\right) \tag{2}$$

$$u\frac{\partial T}{\partial x}+v\frac{\partial T}{\partial y}=\alpha_{\mathrm{nf}}\frac{\partial^2 T}{\partial y^2}+\frac{1}{(\rho c_p)_{\mathrm{nf}}}\left[\mu_{\mathrm{nf}}\left(\frac{\partial u}{\partial y}\right)^2-\frac{\partial q_r}{\partial y}+\sigma B_0^2 u^2\right] \tag{3}$$

$$\begin{aligned} &u=cx, \quad v=-V_0, \quad T=T_w, \quad at \quad y=0\\ &u\to 0, \quad T\to T_\infty \quad as \quad y\to\infty \end{aligned} \tag{4}$$

where y, u, v, T, T_∞, T_w, K, σ, B_0, c_p, and q_r are horizontal co-ordinate, axial velocity, transverse velocity, temperature of the fluid, far field temperature, wall temperature, permeability of porous medium, electrical conductivity, magnetic field coefficient, specific heat, and radiative heat flux in y-direction, respectively.

The nanofluid properties such as the density, ρ_{nf}, the dynamic viscosity, μ_{nf}, thermal diffusivity, α_{nf}, heat capacitance, $(\rho c_p)_{\mathrm{nf}}$, and the thermal conductivity, k_{nf}, are defined in terms of fluid and nanoparticles properties as in [16]:

$$\rho_{\mathrm{nf}}=(1-\varphi)\rho_f+\varphi\rho_n, \qquad \mu_{\mathrm{nf}}=\frac{\mu_f}{(1-\varphi)^{2.5}}, \qquad \frac{k_{\mathrm{nf}}}{k_f}=\frac{k_n+2k_f-2\varphi(k_f-k_n)}{k_n+2k_f+2\varphi(k_f-k_n)}$$

$$(\rho c_p)_{\mathrm{nf}}=(1-\varphi)(\rho c_p)_f+\varphi(\rho c_p)_n, \qquad \alpha_{\mathrm{nf}}=\frac{k_{\mathrm{nf}}}{(\rho c_p)_{\mathrm{nf}}}$$

where ρ_f is the density of fluid, ρ_n – the density of nanoparticles, φ – defined as the volume fraction of the nanoparticles, μ_f – the dynamic viscosity of fluid, $(\rho c_p)_f$ – the thermal capacitance of fluid, $(\rho c_p)_n$ – the thermal capacitance of nanoparticles, and k_f and k_n – the thermal conductivities of fluid and nanoparticles, respectively.

Considering the Rosseland approximation [17] for radiative heat flux, which leads to:

$$q_r=-\frac{4\sigma'}{3\kappa^*}\frac{\partial T^4}{\partial y}$$

where σ' is the Stefan-Boltzmann constant and k^* is the mean absorption coefficient.

If the temperature differences within the flow are sufficiently small such that T^4 may be expressed as a linear function of the temperature, then the Taylor series for T^4 about T_∞, after neglecting higher order terms, is given by:

$$T^4=4T_\infty^3T-3T_\infty^4 \tag{5}$$

In order to solve eqs. (1)-(3), assuming the dimensionless parameters:

$$\begin{aligned} u&=cxf'(\eta)\\ v&=-\sqrt{\vartheta c}f(\eta)\\ \eta&=\sqrt{\frac{c}{\vartheta}}y \end{aligned} \tag{6}$$

where f is a dimensionless stream function and η is the similarity variable.

On applying the similarity transformation parameters and nanofluid parameters, the eqs. (1)-(3) with the boundary conditions (4) changes to:

$$f''' + A_1 f f'' - A_1 f'^2 - A_2 f' = 0 \tag{7}$$

$$\theta'' + B_1 f \theta' + B_2 f''^2 + B_3 f'^2 = 0 \tag{8}$$

$$\begin{aligned} &f = m, \quad f' = 1, \quad \theta = 1, \quad at \quad \eta = 0 \\ &f' \to 0, \quad \theta \to 0, \quad at \quad \eta \to \infty \end{aligned} \tag{9}$$

here non-dimensional parameters are, radiation parameter $N = k^* k_{\mathrm{nf}} / 4\sigma' T_\infty^3$ and $\omega = 1 + (4 / 3N)$, Prandtl number, $\mathrm{Pr} = [\vartheta_f (\rho c_p)_f] / k_f$, Eckert number, $\mathrm{Ec} = c^2 x^2 / [(c_p) f (T_w - T_\infty)]$, magnetic field parameter, $M = \sigma B_0^2 / c\rho_f$, injection parameter, $m = V_0 / (\vartheta_f c)^{1/2}$, dimensionless temperature, $\theta = (T - T_\infty) / (T_w - T_\infty)$:

$$A_1 = \left[(1-\varphi) + \varphi \frac{\rho_n}{\rho_f} \right] (1-\varphi)^{2.5} \qquad A_2 = \frac{1}{K} + (1-\varphi)^{2.5} M$$

$$B_1 = \left[(1-\varphi) + \varphi \frac{(\rho c_p)_n}{(\rho c_p)_f} \right] \left(\frac{k_f}{k_{\mathrm{nf}}} \right) \frac{\mathrm{Pr}}{\omega} \qquad \frac{\mathrm{Ec\,Pr}}{\omega (1 \quad \varphi)^{2.5}} \left(\quad _{\mathrm{nf}} \right) \qquad B_3 = \frac{M\,\mathrm{Pr\,Ec}}{\omega} \left(\frac{k_f}{k_{\mathrm{nf}}} \right)$$

The HPM application:

$$\ell(u) = 0 \tag{10}$$

Boundary conditions,

$$B\left(u, \frac{\partial u}{\partial n} \right) = 0 \tag{11}$$

Here ℓ is a general non-linear differential operator and B is a bounded operator.

To construct a homotopy, the general non-linear operator is divided into two parts; linear, L, and non-linear, N. Hence the eq. (10) changes:

$$L(u) + N(u) = 0 \tag{12}$$

Homotopy that is constructed by He [18-26]:

$$H(v, 0) = L(v) = 0 \tag{13}$$

$$H(v, p) = L(v) + p\, N(v) - (1 - p)\, L(u_0) = 0 \tag{14}$$

where p is homotopy parameter [0, 1].

Homotopy for eqs. (7) and (8):

$$(1-p)(f''' - f_0''') + p\,(f''' + A_1 f\, f'' - A_1 f'^2 - A_2 f') = 0 \tag{15}$$

$$(1-p)(\theta''' - \theta_0''') + p\,(\theta''' + B_1 f\, \theta' + B_2 f''^2 + B_3 f'^2) = 0 \tag{16}$$

The approximation for each of f and θ in terms of the power series of homotopy parameter ρ is written:

$$f = f_0 + p f_1 + p^2 f_2 + p^3 f_3 + \ldots\ldots = \sum_{i=1}^{n} p^i f_i \tag{17}$$

$$\theta = \theta_0 + p\theta_1 + p^2 \theta_2 + p^3 \theta_3 + \ldots\ldots = \sum_{i=1}^{n} p^i \theta_i \tag{18}$$

Substituting eqs. (17) and (18) into eqs. (15) and (16), and comparing the coefficient of like powers of p, the following equations are obtained:

$$\begin{aligned} p^0;\ f_0''' &= 0 \\ \theta_0'' &= 0 \end{aligned} \tag{19}$$

$$f_0'(0)=1,\quad f_0(0)=m,\quad f_0'(\eta_\infty)=0,\quad \theta_0(0)=1,\quad \theta_0(\eta_\infty)=0 \tag{20}$$

$$\begin{aligned} p^1;\ f_1''' + f_0''' - A_1 f_0'^2 - A_2 f_0' + A_1 f_0 f_0'' &= 0 \\ \theta_1'' + B_1 f_0 \theta_0' + B_2 f_0''^2 + B_3 f_0'^2 + \theta_0'' &= 0 \end{aligned} \tag{21}$$

$$f_1'(0)=0,\quad f_1(0)=0,\quad f_1'(\eta_\infty)=0,\quad \theta_1(0)=0,\quad \theta_1(\eta_\infty)=0 \tag{22}$$

$$\begin{aligned} p^2;\ f_2''' - 2A_1 f_0' f_1' - A_2 f_1' + A_1(f_0 f_1'' + f_1 f_0'') &= 0 \\ \theta_2'' + B_1(f_1\theta_0' + f_0\theta_1') + 2B_2 f_0'' f_1'' + 2B_3 f_0' f_1' &= 0 \end{aligned} \tag{23}$$

$$f_2'(0)=0,\quad f_2(0)=0,\quad f_2'(\eta_\infty)=0,\quad \theta_2(0)=0,\quad \theta_2(\eta_\infty)=0 \tag{24}$$

$$\begin{aligned} p^3;\ f_3''' + A_1(f_0 f_2'' + f_1 f_1'' + f_2 f_0'' - f_1^2 - 2f_0' f_1') - A_2 f_2' &= 0 \\ \theta_3'' + B_1(f_0\theta_2' + f_1\theta_1' + f_2\theta_0') + B_2(f_1''^2 + 2f_0'' f_2'') + B_3(f_1'^2 + 2f_0' f_2') &= 0 \end{aligned} \tag{25}$$

$$f_3'(0)=0,\quad f_3(0)=0,\quad f_3'(\eta_\infty)=0,\quad \theta_3(0)=0,\quad \theta_3(\eta_\infty)=0 \tag{26}$$

$$\begin{aligned} p^4;\ f_4''' + A_1(f_0 f_3'' + f_1 f_2'' + f_2 f_1'' + f_3 f_0'' - f_3'^2 - 2f_1' f_2') - A_2 f_3' &= 0 \\ \theta_4'' + B_1(f_0\theta_3' + f_1\theta_2' + f_2\theta_1' + f_3\theta_0') + B_2(2f_1'' f_2'' + f_0'' f_3'') + B_3(f_1' f_2' + f_0' f_3') &= 0 \end{aligned} \tag{27}$$

$$f_4'(0)=0,\quad f_4(0)=0,\quad f_4'(\eta_\infty)=0,\quad \theta_4(0)=0,\quad \theta_4(\eta_\infty)=0 \tag{28}$$

Solutions to these equations are:

$$f_0 = -\frac{1}{10}\eta^2 + \eta + m \tag{29}$$

$$f_1 = \frac{1}{3000}A_1\eta^5 - \frac{1}{120}A_1\eta^4 + \frac{1}{6}A_1\eta^3 - \frac{1}{120}A_2\eta^4 + \frac{1}{6}A_2\eta^3 + \frac{1}{30}A_1 m\eta^3 + \frac{1}{2}T_1\eta^2 \tag{30}$$

$$\begin{aligned} f_2 = {} & \frac{1}{2}\left(\frac{25}{9}A_2^2 + \frac{125}{16}A_1A_2 + \frac{3425}{672}A_1^2 + \frac{5}{48}A_1^2 m - \frac{5}{12}A_1^2 m^2\right)\eta^2 - \frac{1}{3600}A_2^2\eta^6 + \frac{1}{5040000}A_1^2\eta^8 - \\ & - \frac{1}{3600}A_1^2\eta^6 - \frac{1}{126000}A_1^2\eta^7 - \frac{1}{6}A_1 m T_1\eta^3 - \frac{1}{24}A_1^2 m\eta^4 + \frac{1}{24}A_1 T_1\eta^4 + \frac{1}{120}A_1A_2\eta^5 + \\ & + \frac{1}{300}A_1A_2 m\eta^5 + \frac{1}{24}A_2 T_1\eta^4 + \frac{1}{120}A_2^2\eta^5 + \frac{1}{63000}A_1A_2\eta^7 - \frac{1}{300}A_1 T_1\eta^5 - \frac{1}{6000}A_1^2 m\eta^6 - \\ & - \frac{1}{120}A_1^2 m^2\eta^4 - \frac{1}{1800}A_1A_2\eta^6 + \frac{1}{600}A_1^2 m\eta^5 - \frac{1}{24}A_1A_2 m\eta^4 \end{aligned} \tag{31}$$

$$\theta_0 = -\frac{1}{5}\eta + 1 \tag{32}$$

$$\theta_1 = -\frac{1}{600}B_1\eta^4 + \frac{1}{30}B_1\eta^3 + \frac{1}{10}B_1 m\eta^2 - \frac{1}{50}B_2\eta^2 - \frac{1}{300}B_3\eta^4 + \frac{1}{15}B_3\eta^3 - \frac{1}{2}B_3\eta^2 + T_2\eta \quad (33)$$

$$\begin{aligned}\theta_2 = {} & \frac{1}{12}B_1B_3\eta^4 + \frac{1}{120}B_1T_2\eta^4 - \frac{1}{30}B_1^2m^2\eta^3 + \frac{1}{7500}B_2A_1\eta^5 - \frac{1}{300}B_2A_2\eta^4 + \frac{1}{30}B_3T_1\eta^4 + \\ & + \frac{1}{5}B_2T_1\eta^2 + \frac{1}{63000}A_1B_3\eta^7 - \frac{1}{31500}B_1B_3\eta^7 + \frac{1}{120}B_1T_1\eta^4 + \frac{1}{15}B_2A_2\eta^3 - \frac{3}{200}B_1B_3\eta^5 - \\ & - \frac{1}{5000}B_1B_2\eta^5 - \frac{1}{18000}B_1A_1\eta^6 - \frac{1}{2250}B_3A_2\eta^6 - \frac{1}{18000}B_1A_2\eta^6 - \frac{1}{1800}B_3A_1\eta^6 + \\ & + \frac{1}{750}B_1^2m\eta^5 + \frac{1}{300}B_1B_2\eta^4 + \frac{1}{600}B_1A_1\eta^5 + \frac{1}{75}B_3A_1\eta^5 + \frac{1}{600}B_1A_2\eta^5 + \frac{1}{900}B_1B_3\eta^6 + \\ & + \frac{1}{630000}B_1A_1\eta^7 + \frac{1}{15}B_2A_1\eta^3 + \frac{1}{75}B_3A_2\eta^5 - \frac{1}{300}A_1B_2\eta^4 - \frac{1}{40}B_1^2m\eta^4 - \frac{1}{200}B_1^2\eta^5 - \\ & - \frac{1}{63000}B_1^2\eta^7 + \frac{1}{1800}B_1^2\eta^6 - \frac{1}{12}A_2B_3\eta^4 - \frac{1}{6}B_1T_2\eta^3 - \frac{1}{2}B_1mT_2\eta^2 - \frac{1}{12}B_3A_1\eta^4 - \frac{1}{3}B_3T_1\eta^3 - \\ & - \frac{1}{60}B_3A_1m\eta^4 + \frac{1}{3000}A_1B_1m\eta^5 - \frac{1}{60}B_1B_3m\eta^4 + \frac{1}{150}B_1B_2m\eta^3 + \frac{1}{500}B_3A_1m\eta^5 + \\ & + \frac{1}{75}A_1B_2m\eta^3 + \frac{1}{1500}B_1B_3m\eta^5 + \frac{1}{6}B_1B_3m\eta^3 + \left(-\frac{25}{224}B_1B_3 - \frac{425}{1344}B_1^2 + \frac{1}{6}A_1B_2m + \right. \\ & + \frac{1}{12}B_1B_2m - \frac{5}{4}A_1B_3m + \frac{5}{16}A_1B_1m - \frac{125}{36}A_2B_3 - \frac{475}{112}A_1B_3 + \frac{5}{8}B_1B_3m + \frac{5}{12}B_2A_2 + \\ & \left. + \frac{1}{48}B_1B_2 + \frac{13}{24}A_1B_2 + \frac{475}{448}A_1B_1 + \frac{125}{144}A_2B_1 - \frac{5}{12}B_1^2m^2 - \frac{5}{6}B_1^2\right)\eta \end{aligned} \quad (34)$$

Here

$$T_1 = -\frac{15}{8}A_1 - \frac{5}{3}A_2 - \frac{1}{2}A_1m \quad \text{and} \quad T_2 = -\frac{5}{8}B_1 - \frac{1}{2}B_1m + \frac{1}{10}B_2 + \frac{5}{4}B_3$$

Results and discussion

The effects of parameters like volume fraction, porosity parameter, magnetic parameter, injection parameter over the velocity are presented in the figs. 2-5, and the graphical analysis of fluid temperature with respect to volume fraction, radiation parameter, Prandtl number, Eckert number and magnetic parameter is shown in figs. 6-11.

Figures 2 and 3 represent the nanofluid velocity for nanofluids Al_2O_3 and TiO_3, respectively, *vs*. similarity variable, η, for different values of volume fraction, φ, and porosity parameter, K. It is observed that velocity decreases as φ or K increases for both nanofluids, which leads to thinning the momentum boundary-layer. The presence of a porous medium increase resistance to flow and thus reduces fluid velocity. An increase in volume fraction reduces the thickness of nanolayer and dilutes the nanofluid, resulting to reduce the velocity.

Figures 4 and 5 represent the nanofluid velocity for nanofluid Al_2O_3 and TiO_3, respectively, *vs*. η for different values of magnetic parameter, M, and injection parameter, m. The velocity increases with an increase in M or m for both nanofluids. As the magnetic parameter represents the ratio of magnetic injection to the viscous force, therefore, increase in the magnetic field parameter reduces the viscosity of the fluid, that enhances the velocity of the nanofluid. Also an increase in the amount of fluid injected, results in an increase in the velocity boundary-layer.

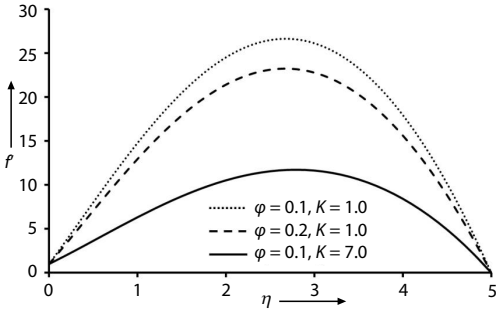

Figure 2. Dimensionless velocity of the nanofluid Al_2O_3 *vs.* η for different values of φ and K when $M = 0.2$, $m = 0.2$, $N = 1.0$, Pr = 1.0, and Ec = 0.1

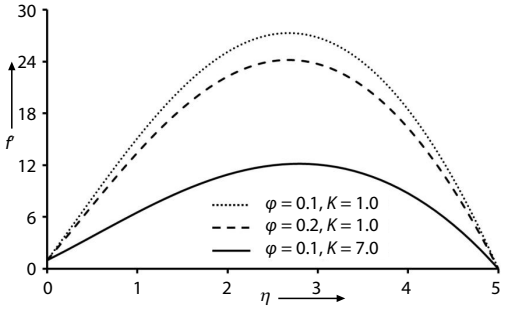

Figure 3. Dimensionless velocity of the nanofluid TiO_3 *vs.* η for different values of φ and K when $M = 0.2$, $m = 0.2$, $N = 1.0$, Pr = 1.0, and Ec = 0.1

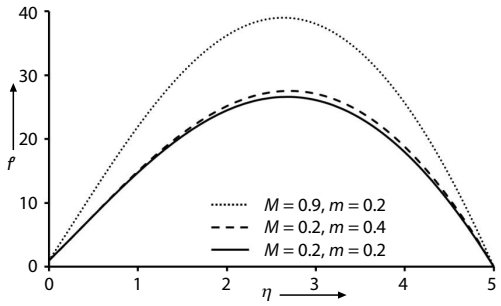

Figure 4. Dimensionless velocity of the nanofluid Al_2O_3 *vs.* η for different values of M and m when $\varphi = 0.1$, $K = 1.0$, $N = 1.0$, Pr = 1.0, and Ec = 0.1

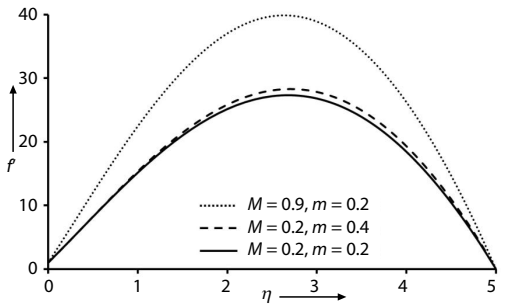

Figure 5. Dimensionless velocity of the nanofluid TiO_3 *vs.* η for different values of M and m when $\varphi = 0.1$, $K = 1.0$, $N = 1.0$, Pr = 1.0, and Ec = 0.1

The dimensionless temperature, θ, is plotted for nanofluid Al_2O_3 and TiO_3, respectively, against η for different values of φ and N, in figs. 6 and 7. It is seen that θ decreases as φ or N increases for both nanofluids. Increasing N reduces the effect of radiation (as radiation is inversely proportional to N), this may be explained by the fact that a decrease in the radiation parameter for a constant k^* and T_∞ implies a decrease in the Rosseland radiation absorptivity, which induces to decrease the thermal boundary-layer thickness.

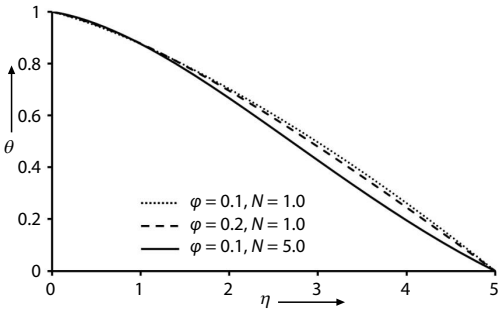

Figure 6. Dimensionless temperature of the nanofluid Al_2O_3 *vs.* η for different values of φ and N when $K = 1.0$, $M = 0.2$, $m = 0.2$, Pr = 1.0, and Ec = 0.1

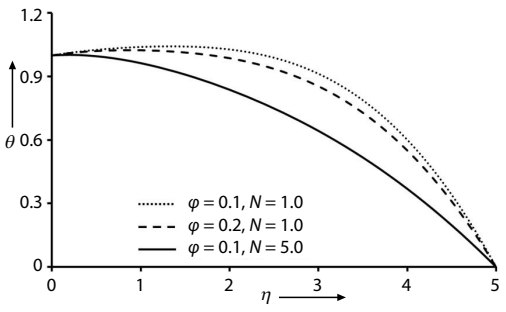

Figure 7. Dimensionless temperature of the nanofluid TiO_3 *vs.* η for different values of φ and N when $K = 1.0$, $M = 0.2$, $m = 0.2$, Pr = 1.0, and Ec = 0.1

Figure 8 represents the dimensionless temperature profile for nanofluid Al_2O_3 to the different values of Prandtl number and M, and in fig. 9 dimensionless temperature is drawn for nanofluid TiO_3 for different values of Prandtl number and M. It has been noticed from these figures that θ increase with an increase of Prandtl number or M for both nanofluids. An increase in Prandtl number increases the viscosity, which increases the temperature due to heat impinging on the surface and magnetic field increases the temperature of the fluid inside the boundary--layer because of excess heating.

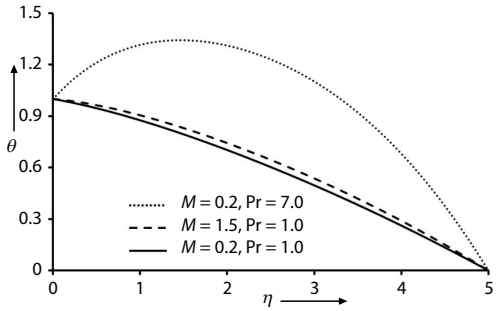

Figure 8. Dimensionless temperature of the nanofluid Al_2O_3 *vs.* η for different values of M and Prandtl number when $\varphi = 0.1$, $K = 1.0$, $m = 0.2$, $N = 1.0$, and Ec = 0.1

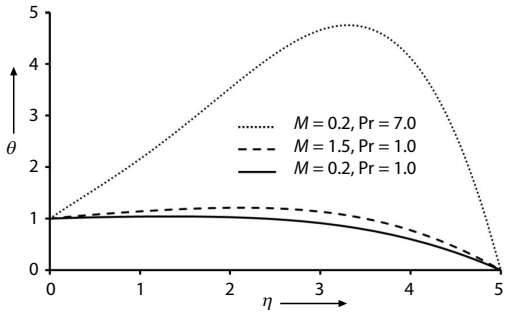

Figure 9. Dimensionless temperature of the nanofluid TiO_3 *vs.* η for different values of M and Pr andtl number when $\varphi = 0.1$, $K = 1.0$, $m = 0.2$, $N = 0.1$, and Ec = 0.1

The dimensionless temperature *vs*. η is drawn for different values of Eckert number to the nanofluids Al_2O_3 and TiO_3 in figs. 10 and 11, respectively. The temperature increases with Eckert number till approximately $\eta = 2.2$, after this point θ reduces as Eckert number increases. Eckert number refers the quantity of mechanical energy converted *via* internal friction to thermal energy which is heat dissipation. Near to the wall, viscous dissipation dominates the heat transfer inside the thermal boundary-layer. Increasing Eckert number causes increase in thermal energy that contribute to heat the regime, and as the nanofluid moves, it changes the conduct and beyond the point $\eta = 2.2$ due to the reversal of heat flow between the surface and surrounding (the nanofluids), the opposite effect is noted, therefore the temperature reduces. This implies that more thermal energy is added to the fluid so that the heat is conducted from plate into the fluid.

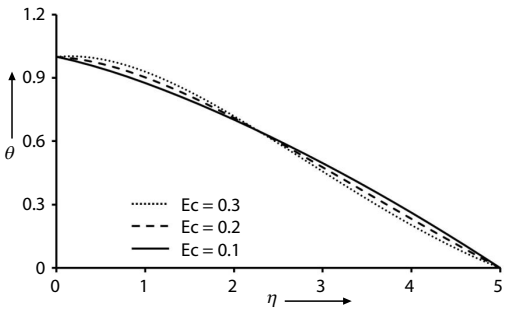

Figure 10. Dimensionless temperature of the nanofluid Al_2O_3 *vs.* η for different values of Eckert number when, $\varphi = 0.1$, $K = 1.0$, $M = 0.2$, $m = 0.2$, $N = 0.1$, and Pr = 1.0

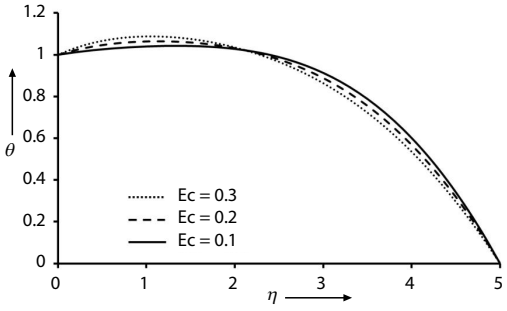

Figure 11. Dimensionless temperature of the nanofluid TiO_3 *vs.* η for different values of Eckert number when, $\varphi = 0.1$, $K = 1.0$, $M = 0.2$, $m = 0.2$, $N = 0.1$, and Pr = 1.0

Conclusions

In the present work flow of an incompressible viscous nanofluid over a stretching porous sheet is taken into account. The governing equations are first transferred to similarity equations, then the obtained coupled equations are changed to recursive ODE by homotopy perturbed analysis method. Finally these equations are solved by using MATLAB. It is observed for both nanofluid (Al_2O_3 and TiO_3) that:

- Effect of porosity or volume fraction is to reduce the velocity boundary-layer.
- Presence of magnetic field increases the velocity boundary-layer.
- Increasing injection parameter enhances the velocity boundary-layer.
- Effect of radiation is to heat up the flow regime, as $\omega = 1 + (4 / 3N)$.
- Increment in Prandtl number or magnetic field extends the thermal boundary-layer.
- Higher volume fraction results in thinner thermal boundary-layer.
- Increase in viscous dissipation increases the thickness of thermal boundary-layer till a certain distance of the sheet $\eta = 2.2$ beyond this point the thermal boundary-layer become thin.

Acknowledgment

The author is very much thankful to Prof. (Ret.) Dr. S. S. Tak, Jai Narain Vyas University, Jodhpur (India) for offering his valuable suggestions and assistance to improve the paper.

References

[1] Choi, S. U. S., Enhancing Thermal Conductivity of Fluids with Nanoparticles, *Proceedings*, ASME International Mechanical Engineering Congress and Exposition, San Francsco, Cal., USA, ASME, FED 231/MD, 1995, pp. 99-105
[2] Wong, K. F. V., Leon, O. D., *Applications of Nanofluids: Current and Future*, Adv. Mech. Eng. Article, ID: 519659, 2010
[3] Khanafer, K., *et al*., Buoyancy-Driven Heat Transfer Enhancement in a Two-Dimensional Enclosure Utilizing Nanofluids, *J. Heat Mass Transfer*, *46* (2003), 19, pp. 3639-3653
[4] Maiga, S. E. B., *et al*., Heat Transfer Enhancement by Using Nanofluids in Forced Convection Flows, *Int. J. Heat Fluid Flow*, *26* (2005), 4, pp. 530-546
[5] Jou, R. Y., Tzeng, S. C., Numerical Research of Nature Convective Heat Transfer Enhancement Filled with Nanofluids in Rectangular Enclosures, *Int. Commun. Heat Transfer*, *33* (2006), 6, pp. 727-736
[6] Tiwari, R. K., Das, M. K., Heat Transfer Augmentation in a Two-Sided Lid-Driven Differentially Heated Square Cavity Utilizing Nanofluids, *International Journal of Heat and Mass Transfer*, *50* (2007), 9-10, pp. 2002-2018
[7] Hwang, K. S., *et al*., Buoyancy-Driven Heat Transfer of Water-Based Al_2O_3 Nanofluids in a Rectangular Cavity, *Int. J. Heat Mass Transfer*, *50* (2007), 19-20, pp. 4003-4010
[8] Oztop, H. F., Abu-Nada, E., Numerical Study of Natural Convection in Partially Heated Rectangular Enclosures Filled with Nanofluids, *International Journal of Heat and Fluid Flow*, *29* (2008), 5, pp. 1326-1336
[9] Muthtamilselvan, M., *et al*., Heat Transfer Enhancement of Copper-Water Nanofluids in a Lid-Driven Enclosure, *Communications in Nonlinear Science and Numerical Simulation*, *15* (2010), 6, pp. 1501-1510
[10] Buongiorno, J., Convective Transport in Nanofluids, *ASME J. Heat Transfer*, *128* (2006), 3, pp. 240-250
[11] Kuznetsov, A. V., Nield, D. A., Natural Convective Boundary-Layer Flow of a Nanofluid Past a Vertical Plate, *Int. J. Therm. Sci*., *49* (2010), 2, pp. 243-247
[12] Abu-Nada, E., Oztop, H. F., Effects of Inclination Angle on Natural Convection in Enclosures Filled with Cu-Water Nanofluid, *International Journal of Heat Fluid Flow*, *30* (2009), 4, pp. 669-678
[13] Gebhart. B., Effects of Viscous Dissipation in Natural Convection, *J. Fluid Mech*., *14* (1962), 2, pp. 225-232
[14] Pantokratoras. A., Effect of Viscous Dissipation in Natural Convection along a Heated Vertical Plate, *Appl. Math*. *Mode*l., *29* (2004), 6, pp. 553-564
[15] Makinde. O. D., Analysis of Sakiadis Flow of Nanofluids with Viscous Dissipation and Newtonian Heating, *Appl*. *Math. Mech*., *33* (2012), 12, pp. 1442-1450

[16] Aminossadati. S. M., Ghasemi. B., Natural Convection Cooling of a Localised Heat Source at the Bottom of a Nanofluid-Filled Enclosure, *European Journal of Mechanics B/Fluids*, *28* (2009), 5, pp. 630-640
[17] Kumar. H., Radiative Heat Transfer with Hydromagnetic Flow and Viscous Dissipation over a Stretching Surface in the Presence of Variable Heat Flux*, Thermal Science*, *13* (2009), 2, pp. 163-169
[18] He. J. H., Non-Perturbative Methods for Strongly Nonlinear Problems, Ph. D. thesis, De-Verlag im Internet GmbH, Berlin, 2006
[19] He. J. H., Some Asymptoticmethods for Strongly Nonlinear Equations, *International Journal of Modern Physics B*, *20* (2006), 10, pp. 1141-1199
[20] He. J. H., Homotopy Perturbation Method for Solving Boundary Value Problems, *Physics Letters A*, *350* (2006), 1-2, pp. 87-88
[21] He. J. H., Application of Homotopy Perturbation Method to Non-Linear Wave Equations, Chaos, *Solitons & Fractals*, *26* (2005), 3, pp. 695-700
[22] He. J. H., Approximate Analytical Solution for Seepage Flow with Fractional Derivatives in Porous Media, *Computer Methods in Applied Mechanics and Engineering*, *167* (1998), 1-2, pp. 57-68
[23] He. J. H., Approximate Solution of Nonlinear Differential Equations with Convolution Product Nonlinearities, *Computer Methods in Applied Mechanics and Engineering, 167* (1998), 1-2, pp. 69-73
[24] He. J. H., Variational Iteration Method – A Kind of Non-Linear Analytical Technique: Some Examples, *International Journal of Non-Linear Mechanics*, *34* (1999), 4, pp. 699-708
[25] He. J. H., Homotopy Perturbation Technique, *Computer Methods in Applied Mechanics and Engineering*, *178* (1999), 3-4, pp. 257-262
[26] He. J. H., A Coupling Method of a Homotopy Technique and a Perturbation Technique for Non-Linear Problems, *International Journal of Non-Linear Mechanics*, *35* (2000), 1, pp. 37-43

Paper submitted: August 31, 2015
Paper revised: July 30, 2016
Paper accepted: August 8, 2016